MULTIPLE MAGNETIC CLOUDS IN INTERPLANETARY SPACE

Y. M. WANG, S. WANG and P. Z. YE

School of Earth and Space Sciences, University of Science and Technology of China, Hefei, China
(E-mail: wym@mail.ustc.edu.cn)

Abstract. An interplanetary magnetic cloud (MC) is usually considered the byproduct of a coronal mass ejection (CME). Due to the frequent occurrence of CMEs, multiple magnetic clouds (multi-MCs), in which one MC catches up with another, should be a relatively common phenomenon. A simple flux rope model is used to get the primary magnetic field features of multi-MCs. Results indicate that the magnetic field configuration of multi-MCs mainly depends on the magnetic field characteristics of each member of multi-MCs. It may be entirely different in another situation. More-over, we fit the data from the *Wind* spacecraft by using this model. Comparing the model with the observations, we verify the existence of multi-MCs, and propose some suggestions for further work.

1. Introduction

Magnetic clouds (MCs) are interplanetary structures, in which the enhanced magnetic field strength, a large and smooth rotation of the magnetic field vector, and low proton temperature can be detected (Burlaga *et al.*, 1981; Osherovich and Burlaga, 1997). The analysis of spacecraft data reveals magnetic clouds as a well-defined subset of coronal mass ejections (CMEs) (Wilson and Hildner, 1984). CMEs associated with erupting filaments are possibly the sources of MCs in interplanetary space (Wilson and Hildner, 1984, 1986; Hundhausen, 1988; Rust, 1994; Bothmer and Schwenn, 1994, 1998). MCs have been studied by many authors because not only are they considered the product of CMEs but they are also important sources of the southward magnetic field. The southward magnetic field is one of the important factors which usually cause geomagnetic storms (Fairfield and Cahill, 1966; Akasofu, 1981; Smith, 1986). As long as the interval of the southward magnetic field is sufficiently long, the solar wind energy will be transferred to the inner parts of the Earth's magnetosphere by magnetic reconnection (Dungey, 1961; Gonzalez *et al.*, 1989). For a single MC, some models have been developed, such as constant-α force-free model (Burlaga, 1988; Lepping, Jones and Burlaga, 1990), toroidally symmetric current loop model (Chen, 1989, 1990; Chen and Garren, 1993; Garren and Chen, 1994), current-core helical flux-rope model (Kumar and Rust, 1996), non-force-free model (Hidalgo *et al.*, 2000, 2002). In these models, all of the primary features of a single MC, such as enhanced field strength, and large-scale rotation of magnetic field's direction, can be clearly described.

As one of the great solar activities, CMEs occur frequently. Especially during the maximum of cycle 23, the rate of the CME occurrence was about 4.17 per day in average [according to the LASCO CME catalog, see *http://cdaw.gsfc.nasa.gov/ CME_list/*]. Since CMEs are likely sources of MCs, occurrences of multiple magnetic clouds (multi-MCs) in the interplanetary medium are expected as well when a CME overtakes another earlier-emitted CME. A study concerning magnetic field features of multi-MCs seems not to be reported yet, but the interaction between a shock and MC has been studied by some authors (e.g., Burlaga, 1991; Vandas *et al.*, 1997). In their work, an overtaking shock penetrates the MC and modifies its parameters. The cloud becomes oblate and its inner magnetic field strength increases during the interaction. However, the primary magnetic field characteristics of the MC are not changed by overtaking shock. In addition, complex ejecta structures have been reported by Burlaga *et al.* (2001) recently. They concluded that some of those complex ejecta were produced by the interaction of two or more CMEs.

This paper makes use of a simple model to analyze some primary magnetic field features of multi-MCs, and compares them with the observations. Although MC was usually led by a shock, we ignore the interaction of shock with MC in our work because it usually could not cause a significant change of primary magnetic field features of MC as mentioned above. We describe the model in the next section and conclude the magnetic field features of multi-MCs in Section 3. In Section 4, a comparison between model and *Wind* data is presented. Finally, we summarize the results and give a discussion.

2. Model Description

Like Kumar and Rust's (1996) work, we model an MC as a current-core helical flux-rope. An MC is considered a twisted flux rope that locally looks like a cylindrical flux rope. Assume that the current flows approximately parallel to the field direction inside MC and that a current-free solution holds outside:

$$\mathbf{j} = \frac{1}{\mu_0} \nabla \times \mathbf{B} = \alpha \mathbf{B} \qquad r \leq r_0 \,, \tag{1}$$

$$\mathbf{j} = \frac{1}{\mu_0} \nabla \times \mathbf{B} = 0 \qquad r > r_0 \,, \tag{2}$$

where r_0 is the radius of flux rope (Figure 1). Similar to the field due to a current-carrying ring, there is no z-component field outside the boundary of MC. Without current sheets at the boundary, the field components are continuous, and $B_z^c = 0$ is obtained at the boundary.

For $r \leq r_0$, we get:

$$\mathbf{B} = \hat{\mathbf{r}} B_r^c + \hat{\theta} B_\theta^c + \hat{\mathbf{z}} B_z^c = \hat{\theta} B_0 J_1(\alpha \mu_0 r) + \hat{\mathbf{z}} B_0 J_0(\alpha \mu_0 r), \tag{3}$$
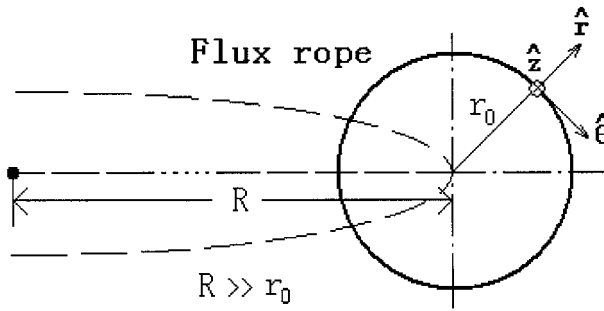
Figure 1. Cross section of flux rope. r_0 is the radius of flux rope and R is the major radius of torus in this model. To describe the model, we use toroidally distorted cylindrical coordinates (r, θ, z) with z along the toroidal axis of the torus.

$$J_0(\alpha\mu_0 r_0) = 0 \,, \tag{4}$$

where J_0 and J_1 are Bessel functions of order 0 and 1, respectively. The superscript 'c' denotes the cylindrical coordinates. The value of $\alpha\mu_0 r_0$ is restricted to be the first zero of J_0 by Equation (4). This is basically the Lundquist solution (Burlaga, 1988; Lundquist, 1950) and we only consider the situation of right-handedness.

The total axial current of the MC is given by

$$I_z^c = \int_0^{r_0} \alpha B_z^c 2\pi r \, dr = \frac{2\pi r_0 B_0}{\mu_0} J_1(\alpha\mu_0 r_0) \,. \tag{5}$$

For $r > r_0$, the field outside the boundary is due to a ring current flowing along the axis of flux rope. Considering an assumption of large-aspect-ratio torus ($R \gg r_0$, R is the major radius of torus, as seen in Figure 1), the flux rope can be treated as a cylindrical system with a current core locally. By assuming the field outside the rope is a consequence of the axial component of the current density, we simplify it to

$$\mathbf{B} = \hat{\theta}\frac{\mu_0 I_z^c}{2\pi r} = \hat{\theta}\frac{r_0 B_0}{r} J_1(\alpha\mu_0 r_0) \,. \tag{6}$$

The field at the boundary satisfies the continuity condition.

In interplanetary space, a MC is usually treated as an independent system. For multi-MCs, we assume that (1) there is no reconnection and no penetration in it, and (2) each member of multi-MCs still maintains the cylindrical form locally although they compress each other. Hence, the total field of multi-MCs is given by

$$\mathbf{B_t} = \sum_{i=1}^{N} \mathbf{B_i} \,, \tag{7}$$

where $\mathbf{B_i}$ denotes magnetic field of one of the multiple magnetic clouds.
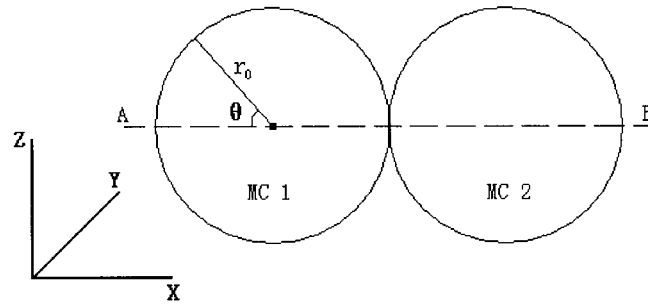
Figure 2. Two-MCs structure. The radii r_0 of flux ropes are the same. The Cartesian coordinates are used to describe the magnetic field. X-axis parallels the path $\overline{AB}$, which passes through the center of both clouds, and Z-axis is in the plane and vertical to $\overline{AB}$.

3. Magnetic Field Features of Multi-MCs in the Model

To obtain the general field features of multi-MCs in this model, we assume that the multi-MCs consists of two parallel MCs. The magnetic field strength and size of them are the same. They just touch each other and still remain in cylindrical configuration locally (Figure 2). In order to be convenient for comparing the model with the observations, we use Cartesian coordinates (as seen in Figure 2) to describe the magnetic field of multi-MCs hereafter. From Equations (3), (6), and (7), we obtain the total magnetic field strength of multi-MCs

$$B = |\mathbf{B_t}| = \left| \sum_{i=1}^{N} \mathbf{B_i} \right| = \sqrt{\left(\sum_{i=1}^{N} B_{i\theta}^c \sin\theta \right)^2 + \left(\sum_{i=1}^{N} B_{i\theta}^c \cos\theta \right)^2 + \left(\sum_{i=1}^{N} B_{iz}^c \right)^2}, \quad (8)$$

and z component field (i.e., northward component of magnetic field),

$$B_z = \sum_{i=1}^{N} B_{i\theta}^c \cos\theta , \qquad (9)$$

where the index 'i' refers to the each member of the multi-MCs.

By assuming the observational path to be along the path $\overline{AB}$, we get the results as shown in Figure 3. The curves in Figures 3(a) and 3(b), where $\overline{AB}$ just passes through the center of both clouds, present two different situations respectively. In Figure 3(a), the field lines of each MC rotate in the same direction. The value of B reaches a maximum near the center of each cloud, and declines to the lowest value between the two MCs. The B_z goes through two fluctuations and forms four extremum points. The absolute values of the middle two extremum points (marked by '2', '3' in the second panel of Figure 3(a)) are obviously smaller than the other two (marked by '1', '4'). On the other hand, in Figure 3(b), the field lines of each cloud rotate in the opposite direction. The values of B and B_z are symmetrical relative to the joint. The total field B also reaches a peak near the center of each
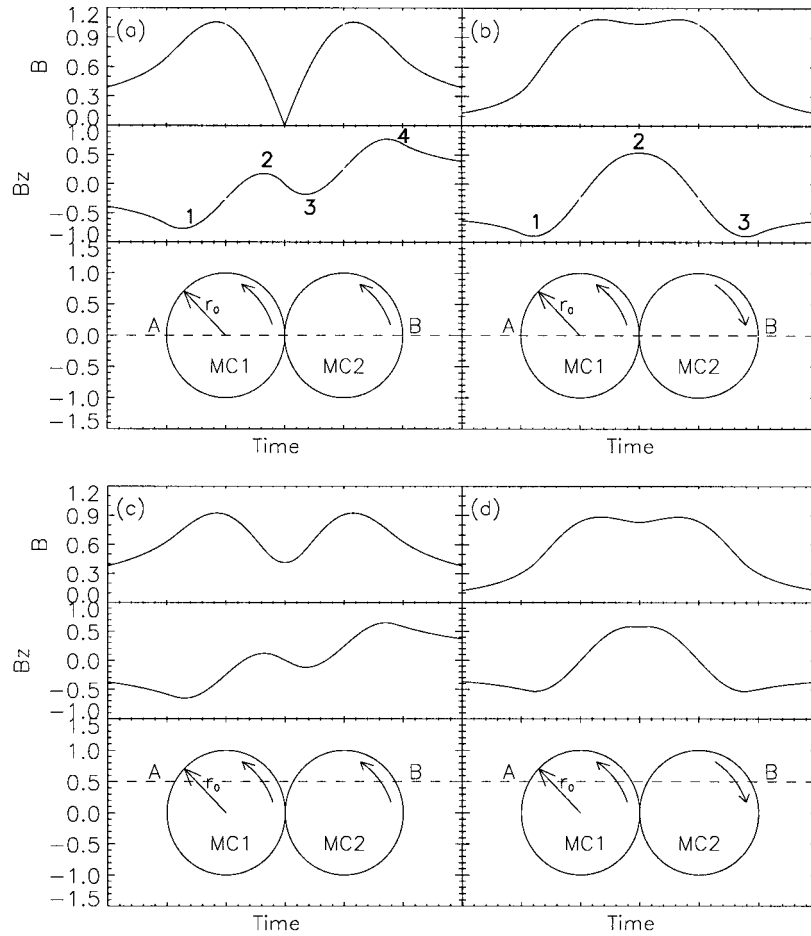
Figure 3. Two-MCs structure with (a, c) same twist and (b, d) opposite twist. *From top to bottom* are plotted: magnetic field strength B, z component field B_z, and cross section of flux ropes in model. The observational path is along the path $\overline{AB}$, and in (a, b) the path $\overline{AB}$ just passes through the center of the clouds. The numbers marked in this figure denote the extremum points of B_z.

cloud but only forms a dimple at the joint. The B_z forms three extremum points: two are minor and the middle one is very large and dominating (marked by '1', '2', '3' in the second panel of Figure 3(b)). As a further illustration, Figures 3(c) and 3(d) describe another situation, in which the observational path $\overline{AB}$ does not pass through the center of the clouds. It is obvious that these curves in Figures 3(c) and 3(d) are similar to those in Figures 3(a) and 3(b) except that the amplitude becomes smaller. Certainly, the characteristics of the magnetic field will be different for other situations. For example, if two clouds are not the same, or they are inclined to the ecliptic.

Two-MCs structure is the simplest case of multi-MCs. As for three, four or even more MCs systems, the situation must be more complicated. For instance, there

will be four peaks of total field strength **B** and four fluctuations of B_z in a typical four-MCs structure if each member has the same magnetic energy and rotates in the same direction. Evidently, the configuration of magnetic field of multi-MCs is much different from that of a single MC.

4. Compared with Observations

4.1. OBSERVATIONS

The *Wind* spacecraft observed a MC-like structure in the solar wind during 26–27 November 2000 (Figure 4). This structure began at about 13:00 UT on 26 November and seemingly ended at about 12:30 UT on 27 November (marked by 'A', 'B', respectively, in Figure 4), which lasted approximate one day. The structure was led by two shocks 'S1' and 'S2' (as marked in fifth panel). The first shock 'S1' caused a small peak in *B* and enhancement of density. We think that it was another individual ejecta possibly. Meanwhile, it is possible that the shock 'S2' was produced by several overtaking shocks merging (Burlaga, 2001). Because we only consider the MCs themselves but not shocks, we exclude this leading part from our study.

At the inner of this structure, the total field strength *B* did not always increase and its component fields fluctuated fiercely and regularly. There were four peaks of *B* and roughly four slight fluctuations of solar wind speed *V*. We suppose that this structure was a multi-MCs, which was made out of four MCs. We separate this structure into four parts (as seen in Figure 4) according to the basic fluctuations of *B*. The size of the middle two parts was smaller than that of others due to being compressed from both sides. From Figure 4 we can find that the field strength of each part enhanced, the corresponding field direction varied regularly, and the proton temperature in each part was low, too. These are all defining characteristics of a MC.

To verify our speculation determine the corresponding CMEs, we use the maximum solar wind flow speed during that interval to estimate the time of potential CMEs initiation. This method was used by Lindsay *et al.* (1999) to identify the solar-terrestrial events. According to the *Wind* data, the maximum solar wind speed was about 670 km s^{-1} in the structure. We estimate that CMEs should occur approximately 62 hours earlier by supposing uniform motion of CMEs in interplanetary space. Thus, we consider that the CMEs, which erupted around 24 November, should be the sources of this interesting multi-MCs structure. From 24 to 25 November, there were six Earth-directed halo CMEs (Nitta and Hudson, 2001), which first appeared in LASCO/C2 at 05:30 UT on 24th, 15:30 UT on 24th, 22:06 UT on 24th, 01:32 UT on 25th, 09:30 UT on 25th, and 19:31 UT on 25th, respectively. The first three and last one of them were identified as homologous CMEs (Zhang and Wang, 2001). All of these homologous CMEs initiated from the same active
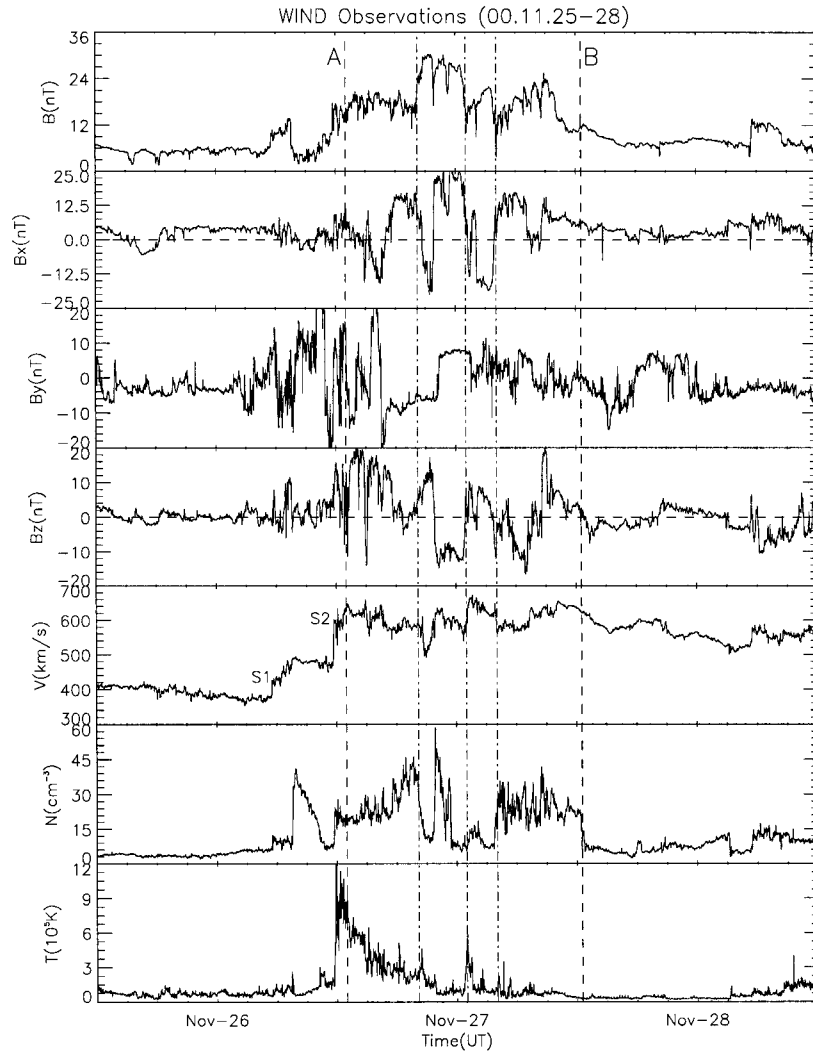
Figure 4. Observations by the *Wind* spacecraft from 25 November (12:00 UT) to 28 November 2000 (12:00 UT). From *top* to *bottom* are plotted: magnetic field strength *B*, $x/y/z$ component field B_x, B_y, B_z, solar wind speed *V*, proton density *N*, and the proton temperature *T*. *Vertical dashed lines* denote, *from left to right*, the times of the structure's beginning and ending. *Vertical dash-dot lines* denote the borders of each member MC in the structure.

region. Each member of them associated with a member of homologous flares. Their extended EUV dimmings and the coronagraph appearances were similar too. We think that these properties are favorable to cause a typical multi-MCs. According to Table 1 in Nitta and Hudson's (2001) paper, the projected speed of six halo CMEs were approximate 711 km s^{-1}, 890 km s^{-1}, 935 km s^{-1}, 2202 km s^{-1}, 610 km s^{-1}, 596 km s^{-1} respectively. Obviously, among the first four CMEs, the latter moved faster than the former. Thus, they were able to form the four-MCs
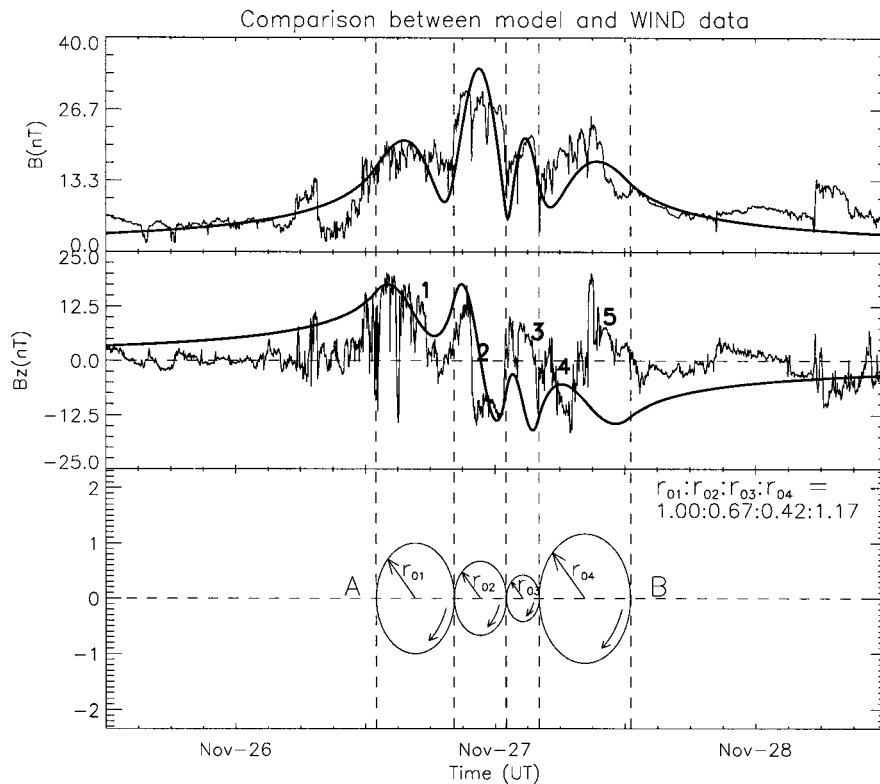
Figure 5. Comparison between the four-MCs model and *Wind* data. *Vertical dashed lines*, which are the same as those in Figure 4, denote the borders of each cloud. The numbers '1–5' mark the five observed fluctuations in the studied structure. Fitting curve is calculated by four-MCs model along path $\overline{AB}$.

structure in interplanetary space. Moreover, no other halo CMEs were observed by LASCO around 24 November.

Combined with *Wind* observations at 1 AU, we think that the multi-MCs did contain four MCs (as shown by Figure 5) and they were correlated with the first four halo CMEs mentioned above. The first three clouds were caused by homologous CMEs occurred on 24 November and the last cloud was not produced by one of the homologous CMEs but the halo CME that occurred at 01:32 UT on 25 November because the other halo CMEs were too late and too slow to chase earlier ones. In addition, it is probable that the compression region ahead of each cloud had become more minor and ignorable relative to the cloud itself due to the interaction between the MCs. In the next subsection, we model four-MCs system to further verify our viewpoint.

4.2. COMPARISON

According to the above analysis, we get the following assumptions at 1 AU: (1) there were four MCs in the structure with same rotating direction; (2) these MCs still maintained the cylindrical configuration locally although they compressed each other and could not expand freely; (3) the axes of flux ropes were parallel to each other and lay in the same plane; (4) the observational path was along the $\overline{AB}$ (as seen in Figure 5). Moreover, we do not consider the situation of the clouds inclined to the ecliptic. Due to these assumptions, we only attempt to fit the total magnetic field strength B.

To fit the model to *Wind* observations, we made half-hourly averages of the magnetic field data and applied a least-squares program that uses the Levenberg–Marquardt algorithm (Marquardt, 1963). The following equation is adopted to calculate goodness-of-fit.

$$\chi^2 = \Sigma(B - B^f)^2/N , \tag{10}$$

where B is the observational data of total field, B^f is the fitting data, and N is the number of field vectors. The B and B^f are unit normalized. We obtain the final estimates for the four free parameters: B_0 of each MC: B_{01}, B_{02}, B_{03}, B_{04} are 16.84, 34.24, 18.60, 13.29, respectively, and χ^2 is 0.027, which indicates a good fit.

As shown in Figure 5, we find that the four peaks of the fitting curve in the first panel are very consistent with *Wind* data. The correlation between the fitting data and observed data is significant at the confidence level 99% with a correlation coefficient about 0.695. This result also implies that the complex structure is a four-MCs system. As further comparison, we plot the corresponding fitting curve of the z-component B_z in second panel. The correlation in B_z is not very good and the values of the fitting B_z deviate greatly from the observational results. The weak correlation and deviation are possibly caused by too many simplifications and assumptions in the model, for example, we did not consider the clouds inclination to the ecliptic and ignored the complicated interaction between the clouds. Comparing the B_z fitting curve with *Wind* data, we find that there are five fluctuations (marked by numbers '1–5' in Figure 5) observed in this structure but there are only four in the fitting curve. As seen in the second panel, the first three fluctuations correspond well. The difference of fluctuations primarily happened in the last cloud. We think the reason is that the last MC did not belong to the homologous CMEs and was located at the tail of this multi-MCs structure where it was easier to be affected by ambient solar wind. Due to the more complicated facts, the model only indicates the primary features of magnetic field of this four-MCs structure.

5. Summary and Discussion

We use a simple model to analytically describe the primary magnetic field features of multi-MCs. By analyzing a complex structure observed on 26–27 November and comparing the model with the *Wind* data, we verify the existence of multi-MCs in interplanetary space. The reason why the complex structure is a four-MCs system is summarized as follows: (1) Each part of the structure is primarily consistent with the criteria of magnetic cloud (e.g., Burlaga, 1988). (2) The number of the clouds is the same as the number of the corresponding halo CMEs. Around 24 November, there were just four Earth-directed halo CMEs, of which the initial projected speeds formed an incrementing sequence. (3) The model is in rough agreement with the observations. Especially for total field strength B, the fitting curve is well consistent with the *Wind* data.

The example mentioned in this paper is very intricate. In fact, the complex structure did not end at 12:30 UT on 27 November. There was another MC-like structure following it obviously because in addition to the four halo CMEs, which are thought to be the sources of the multi-MCs, there were still two halo CMEs and four non-halo CMEs observed on 25 November. The high rate of CMEs' occurrence causes the more complicated structure in interplanetary space. Moreover, although we can distinguish the properties of MC from this multi-MCs structure, these characteristics have become more ambiguous and more indeterminable. The interaction between clouds, including reconnection and penetration, greatly affects the cloud configuration, intrinsic field properties, and so on.

Under the effect of an overtaking shock, the magnetic field strength usually increases inside the cloud (e.g., Burlaga, 1991; Vandas *et al.*, 1997). However, in multi-MCs structure, the strength does not always rise. The southward component of field, which is usually thought to be the major cause of geomagnetic storms (e.g., Dungey, 1961; Akasofu, 1981; Gonzalez *et al.*, 1994), may also increase or decrease. So the effect on the Earth's magnetosphere can certainly be expected to be different accordingly. These variation mainly lie on the rotating direction of each member of multi-MCs and the energy they contain. Furthermore, we can estimate the compressed degree of each member of multi-MCs. For the instance mentioned above, the middle two clouds were compressed much more greatly than the other two. Hence, the interval of corresponding southward field was also shortened considerably. This certainly affected the amplitude of geomagnetic disturbance.

Due to the high occurrence of CMEs during solar maximum, multi-MCs should be believed a frequent phenomenon in interplanetary space. This paper utilizes a flux rope model with many simplified conditions to describe the properties of the multi-MCs system. It can only reveal basic features but not details. Specifically, the interaction between the MCs cannot be obtained by the current method. Further research should rely on numerical simulation.

Acknowledgements

References

Akasofu, S. -I.: 1981, *Space Sci. Rev.* **28**, 121.

Bothmer, V. and Schwenn, R.: 1994, *Space Sci. Rev.* **70**, 215.

Bothmer, V. and Schwenn, R.: 1998, *Ann. Geophys.* **16**, 1.

Burlaga, L.: 1988, *J. Geophys. Res.* **93**, 7217.

Burlaga, L.: 1991, in R. Schwenn and E. Marsch (eds.), *Physics of the Inner Heliosphere II, Particles, Waves and Turbulence, Physics and Chemistry in Space 21, Space and Solar Physics*, Springer-Verlag, New York, p. 1.

Burlaga, L., Sittler, E., Mariani, F. and Schwenn, R.: 1981, *J. Geophys. Res.* **86**, 6673.

Burlaga, L., Skoug, R. M., Smith, C. W., Webb, D. F., Zurbuchen, T. H. and Reinard, A.: 2001, *J. Geophys. Res.* **106**, 20957.

Chen, J.: 1989, *Astrophys. J.* **338**, 453.

Chen, J.: 1990, in C. T. Russell, E. R. Priest and L. C. Lee (eds.), *Physics of Magnetic Flux Ropes, Geophys. Monogr. Ser.*, AGU, Washington, DC, **58**, 269.

Chen, J. and Garren, D. A.: 1993, *Geophys. Res. Lett.* **20**, 2319.

Dungey, J. W.: 1961, *Phys. Rev. Lett.* **6**, 47.

Fairfield, D. H. and Cahill, L. J.: 1966, *J. Geophys. Res.* **71**, 155.

Garren, D. A. and Chen, J.: 1994, *Phys. Plasmas* **1**, 3425.

Gonzalez, W. D., Joselyn, J. A., Kamide, Y., Kroehl, H. W., Rostoker, G., Tsurutani, B. T. and Vasyliunas, V. M.: 1994, *J. Geophys. Res.*, **99**, 5771.

Gonzalez, W. D., Tsurutani, B. T., Gonzalez, A. L. C., Smith, E. J., Tang, F. and Akasofu, S. I.: 1989, *J. Geophys. Res.* **94**, 8835.

Hidalgo, M. A., Cid, C., Medina, J. and Vinas, A. F.: 2000, *Solar Phys.* **194**, 165.

Hidalgo, M. A., Cid, C., Vinas, A. F. and Sequeiros, J.: 2002, *J. Geophys. Res.* **107(A1)**.

Hundhausen, A. J.: 1988, *Solar Wind Six, Technical Note NCAR/TN Proc.* **306**, 181.

Kumar, A. and Rust, D. M.: 1996, *J. Geophys. Res.* **101**, 15667.

Lepping, R. P., Jones, J. A. and Burlaga, L. F.: 1990, *J. Geophys. Res.* **95(A8)**, 11957.

Lindsay, G.M., Luhmann, J. G., Russell, C. T. and Gosling, J. T.: 1999, *J. Geophys. Res.* **104**, 12515.

Lundquist, S.: 1950, *Ark. Fys.* **2**, 361.

Marquardt, D. W.: 1963, *J. Soc. Ind. Appl. Math.* **11**, 431

Nitta, N. V. and Hudson, H. S.: 2001, *Geophys. Res. Lett.* **28**, 3801.

Osherovich, V. and Burlaga, L. F.: 1997, in N. Crooker, J. A. Joselyn and J. Feynman (eds.), *Coronal Mass Ejections, Geophys. Monogr. Ser. AGU* **99**, 157.

Rust, D. M.: 1994, *Geophys. Res. Lett.* **21**, 241.

Smith, E. J., Slavin, J. A., Zwickl, R. D. and Bame, S. J.: 1986, in Y. Kamide and J. A. Slavin (eds.), *Solar Wind-Magnetoshpere Coupling*, Terra Scientific, Tokyo, p. 345.

Vandas, M., Fischer, S., Dryer, M., Smith, Z., Detman, T. and Geranios, A.: 1997, *J. Geophys. Res.* **102**, 22295.

Wilson, R. M. and Hildner, E.: 1984, *Solar Phys.* **91**, 168.
Wilson, R. M. and Hildner, E.: 1986, *J. Geophys. Res.* **91**, 5867.
Zhang, J. and Wang, J.: 2002, *Astrophys. J.* **566**, L117.